

Review of VCSELs for Complex Data-Format Transmission Beyond 100-Gbit/s

Chih-Hsien Cheng , *Member, IEEE*, Wei-Chi Lo, Borching Su , *Member, IEEE*,
Chao-Hsin Wu , *Senior Member, IEEE*, and Gong-Ru Lin , *Fellow, IEEE*

(Invited Paper)

Abstract—Persistent efforts on developing advanced and complex data algorithms to enable the vertical-cavity surface-emitting lasers (VCSELs) for data beyond 100-Gbit/s has been reviewed in this paper. This endeavor not only elevates the bit rate of the IEEE802.3 standards for data center applications but also to initiate the unification of data format for wired and wireless network coverage. To date, the highest allowable data rates of the single-VCSEL-based optical link are 80 Gbit/s for the NRZ-OOK format under back-to-back (BtB) transmission 168 Gbit/s for the PAM-4 format over 150-m OM5 MMF, and the 224 Gbit/s for the QAM-OFDM format at BtB case. For the high-level complex data-format transmission with rigorous demand on the signal-to-noise ratio (SNR), this work demonstrates the most up-to-date 32-ray quadrature amplitude modulation generalized frequency division multiplexing (32-QAM GFDM) data algorithm with optimized amplitude and K value for encoding the multimode (MM) VCSEL. To achieve the higher spectral-usage efficiency based on the SNR spectrum for maximal transmission data rate, the bit-loading discrete multi-tone (DMT) technique is implemented by rearranging each subcarrier to the appropriate QAM levels. By utilizing 32-QAM GFDM and bit-loading DMT, the maximal data rate in the BtB case could respectively achieve 119.5 Gbit/s and 130 Gbit/s when operating the MM VCSEL at 55 °C. The transmission capacity of the VCSEL operated at 55 °C would decrease to 93.8 Gbit/s for 32-QAM GFDM and 83 Gbit/s for bit-loading DMT after propagating through OM5 MMF with modal dispersion.

Index Terms—Vertical-cavity surface-emitting laser (VCSEL), multimode fiber (MMF), non-to-zero on-off keying (NRZ-OOK), 4-level pulse amplitude modulation (PAM-4), quadrature amplitude modulation orthogonal frequency division multiplexing (QAM-OFDM), quadrature amplitude modulation generalized frequency division multiplexing (QAM-GFDM), bit-loading, discrete multi-tone (DMT).

Manuscript received June 18, 2021; revised August 1, 2021; accepted August 9, 2021. Date of publication August 13, 2021; date of current version September 15, 2021. This work was supported by the Ministry of Science and Technology, Taiwan, under Grants MOST 109-2221-E-002-184-MY3, MOST 110-2221-E-002-100-MY3, MOST 110-2124-M-A49-003-, and MOST 110-2224-E-992-001-. (Corresponding author: Gong-Ru Lin.)

Chih-Hsien Cheng is with the Graduate Institute of Photonics and Optoelectronics, National Taiwan University, Taipei 10617, Taiwan, and also with the Research Center for Advanced Science and Technology, University of Tokyo, Tokyo 153-0041, Japan.

Wei-Chi Lo, Chao-Hsin Wu, and Gong-Ru Lin are with the Graduate Institute of Photonics and Optoelectronics and Department of Electrical Engineering, National Taiwan University, Taipei 10617, Taiwan (e-mail: grlin@ntu.edu.tw).

Borching Su is with the Graduate Institution of Communication Engineering, National Taiwan, Taipei 10617, Taiwan.

Digital Object Identifier 10.1109/JPHOT.2021.3104647

I. HISTORICAL REVIEW ON THE PROGRESS OF VCSEL BASED MULTIPLE DATA-FORMAT TRANSMISSION

OWING to the development of the Internet of Things (IoT) in recent years, the optical fiber transmission carried by the various laser diodes such as the Fabry-Perot laser diode (FPLD), the distributed feedback laser diode (DFBLD), and the vertical-cavity surface-emitting laser (VCSEL) starts to study. Not only the long-reached (the long-haul backbone and the metropolitan area networks) but also short-reached (the intra/inter-data center networks and area link) optical links can be demonstrated via the combination of the LD and optical fiber. The demand for broadband voice and high-quality video data becomes more important in recent years. The internet-related industry develops the related high-speed transmission including the cloud storage network, intra/inter-data center networks, and the fiber-to-the-home link to integrate the wired and wireless network. From the abovementioned description, the high data rate in the cloud storage network or intra/inter-data center networks becomes a key issue in the future. The optical link based on the combination of the multimode (MM) VCSEL and multimode fiber (MMF) can be regarded as one of the solutions for data-center applications because the VCSEL exhibits a low-threshold current, high power conversion efficiency, and low power consumption. Therefore, the related communication standards for the VCSEL-MMF link at or beyond 400 Gbit/s start to be build up. In 2017, IEEE802.3cm standard announced the 400 Gbit/s transmissions over 16 850-nm VCSEL-MMF lanes in 400GBASE-SR16 specification [1]. In 2020, the data rate should be increased to 50 Gbit/s per channel for the 400GBASE-SR8 specification in IEEE 802.3 cm [2]. In the 400GBASE-SR4.2 specification, the 850-nm and 910-nm VCSELs are utilized to improve the data rate to 100 Gbit/s per channel [2]. In addition to IEEE 802.3 Working Group, the Shortwave Wavelength Division Multiplexed Multi-Source Agreement (SWDM MSA) group also developed the 40G SWDM4 [3] and 100G SWDM4 [4] standards to demonstrate the VCSEL-based transmission over different-type MMFs. According to the 2018 Ethernet Roadmap from Ethernet Alliance [5], the Ethernet speed can be achieved to 800 Gbit/s or 1.6 Tbit/s in 2022. In recent years, Finisar and VI-Systems companies further demonstrate the 100-Gbit/s SWDM4 optical transceiver over 100 m. Therefore, the

high-speed VCSEL becomes the most important light source of the short-reached data-center networks.

A. Encoding the VCSEL With the NRZ-OOK Format for Data-Center Applications

During the past two decades, various researches about the VCSELs carrying the simplest non-return-to-zero on-off keying (NRZ-OOK) data format were reported to initiate the short-reached data-center applications from many academic research groups. In 2007, Chang and co-workers used the 35-Gbit/s NRZ-OOK data stream to directly modulate the tapered-oxide-apertured 980-nm VCSEL with a data-rate/power-dissipation of 3.5 Gbit/s/mW [6]. In 2008, Shi's group utilized the Zn-diffusion technology to form the single-mode (SM) VCSEL with a modulation current efficiency of 8.2 GHz/mA [7]. This Zn-diffused SM VCSEL also transmitted the 10-Gbit/s NRZ-OOK data with a data-rate/power-dissipation ratio of 6.5 Gbit/s/mW [7]. Moreover, the large-aperture VCSEL with a modulation bandwidth of 20 GHz was fabricated by Westbergh *et al.* to perform the 25-Gbit/s NRZ-OOK transmission [8]. In 2009, the 40-Gbit/s NRZ-OOK data carried by the oxide-confined VCSEL was demonstrated by Blokhin *et al.* [9]. Hatakeyama and co-workers designed the strain-compensated multiple quantum wells in an InGaAs/GaAsP VCSEL to achieve the 25-Gbit/s NRZ-OOK transmission under 100 °C operation [10]. After 2010, the related reports about the data transmission were emphasized on not only the back-to-back (BtB) case but also different-length MMF conditions. In 2010, Choquette *et al.* used the holey structure in VCSEL via implantation to achieve the optical confinement [11]. This VCSEL with the hole structure can deliver the 25-Gbit/s NRZ-OOK data over 104-m MMF [11]. Zhu and co-workers utilized the 100-m seven-core MMF, tapered MMF connector, and 850-nm VCSELs to achieve the NRZ-OOK transmission with a total data rate of 70 Gbit/s [12]. In 2011, Moser's group demonstrated that the oxide-confined VCSEL transmitted the 17-Gbit/s and 25-Gbit/s NRZ-OOK data over 100-m MMF with dissipation-power-efficiencies of 69 fJ/bit and 99 fJ/bit, respectively [13]. The 25-Gbit/s NRZ-OOK transmission with a dissipated-energy-to-bit-rate ratio of 122.4 mW/Tbits carried by a small spectral-linewidth VCSEL over 300-m MMF link was demonstrated by Fioi *et al.* [14]. In 2012, Westbergh and co-workers demonstrated the NRZ-OOK transmission at 47 Gbit/s in BtB case and at 44 Gbit/s over 50-m OM4 MMF link carried by the 7- μ m-oxide-confined VCSEL with a modulation bandwidth of 28 GHz [15]. Lott *et al.* directly modulated the VCSEL to transmit the 25-Gbit/s NRZ-OOK data over 500-m OM3 MMF [16]. Safaisini and co-workers combined with an 850-nm VCSEL and an integrated mode filter to transmit the NRZ-OOK data at 25 Gbit/s in 1.3-km MMF and 20 Gbit/s at 2-km MMF for achieving a bitrate-distance product of 40 Gbit/s-km [17]. In 2014, Moser *et al.* operated the 980-nm VCSEL at 85 °C to demonstrate the 46-Gbit/s NRZ-OOK transmission under the error-free criterion [18]. Later on, the breakthrough on the VCSEL-based optical link beyond 50-Gbit/s data transmission keeps pace with the rapid development of high-speed data centers. Lott *et al.*

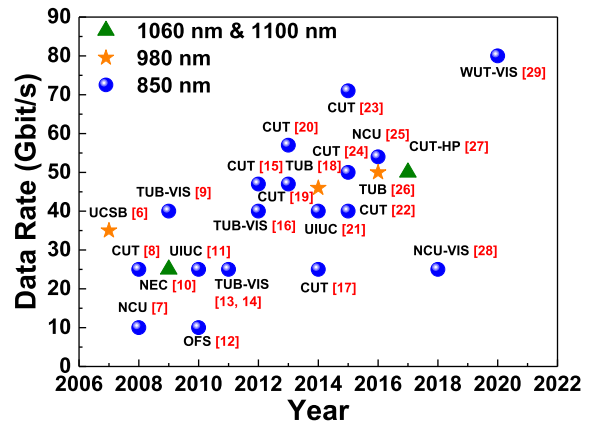


Fig. 1. The developing progress on the transmission rate of NRZ-OOK data format carried by the VCSEL.

enhanced the modulation efficiency and impedance matching of the VCSEL via the diameter variation of the oxide-confined aperture to respectively deliver the NRZ-OOK data at 55 Gbit/s and 43 Gbit/s in BtB and 100-m OM4 MMF cases [19]. They also optimized the photon lifetime in VCSEL to achieve the NRZ-OOK transmission at 57 Gbit/s in BtB case, 55 Gbit/s over a 50-m MMF link, and 43 Gbit/s over 100-m MMF link [20]. Tan *et al.* demonstrated that the 850-nm VCSEL with an oxide aperture diameter of 4 μ m exhibited the relative intensity noise of 154.3 dB/Hz to perform the 40-Gbit/s NRZ-OOK transmission with an energy/data efficiency of 341 fJ/bit [21].

In 2015, six 850-nm VCSELs carrying the 40-Gbit/s NRZ-OOK data were utilized by Westbergh *et al.* to form the dense 2-D six-channel VCSEL array for achieving an aggregate transmission capacity of 240 Gbit/s over a multicore fiber [22]. Kuchta *et al.* employed the BiCMOS-driver IC with feed-forward equalization to optimize the NRZ-OOK transmission performance with a data rate of 71 Gbit/s [23]. Haglund reported that the 850-nm VCSEL with a modulation bandwidth of 30 GHz delivered the 50-Gbit/s NRZ-OOK transmission with dissipated heat energy of 95 fJ/bit [24]. In 2016, Chi *et al.* obtained the quasi-SM VCSEL with an analog bandwidth of 27 GHz via the Zn-diffusion technology and oxide-relief aperture to transmit the NRZ-OOK data at 54 Gbit/s with a bit-error-rate (BER) of 1.4×10^{-4} over 1-km OM4 MMF [25]. Moreover, Larisch *et al.* changed the VCSEL temperature to 85 °C without external cooling to maintain the data rate of the NRZ-OOK transmission at 50 Gbit/s [26]. In 2017, Simpanen *et al.* fabricated the oxide-confined VCSEL to demonstrate the 50-Gbit/s NRZ-OOK transmission with an energy dissipation of 100 fJ/bit [27]. In 2018, Ledentsov *et al.* operated the VCSEL temperature at 150 °C to allow the 25-Gbit/s NRZ-OOK transmission [28]. In 2020, Chorchos and co-workers demonstrated the NRZ-OOK transmission carried by the 850-nm VCSEL at 80 Gbit/s over 2-m MMF and 72 Gbit/s over 50-m MMF [29]. From the previous reports about the NRZ-OOK data transmission in Fig. 1 and Table I, the data rate of the NRZ-OOK transmission hardly achieves 100 Gbit/s because the NRZ-OOK data has a low spectral usage efficiency. Only one method to achieve the data

TABLE I
LUMINESCENT WAVELENGTH AND BIT RATES OF THE NRZ-OOK
TRANSMISSION CARRIED BY THE VCSEL

Group	Wavelength (nm)	Bit Rate (Gbit/s)	Year [Ref]
UCSB	980	35	2007 [6]
NCU	850	10	2008 [7]
CUT	850	25	2008 [8]
TU Berlin-VI Systems	850	40	2009 [9]
NEC	1100	25	2009 [10]
UIUC	850	25	2010 [11]
OFS	850	10 (Single) 70 (Array)	2010 [12]
TU Berlin-VI Systems	850	25	2011 [13]
TU Berlin-VI Systems	850	25	2011 [14]
CUT	850	47	2012 [15]
TU Berlin-VI Systems	850	40	2012 [16]
CUT	850	25	2014 [17]
TU Berlin	980	46	2014 [18]
CUT	850	47	2013 [19]
CUT	850	57	2013 [20]
UIUC	850	40	2014 [21]
CUT	850	40 (Single) 240 (Array)	2015 [22]
CUT	850	71	2015 [23]
CUT	850	50	2015 [24]
NCU	850	54	2016 [25]
TU Berlin	980	50	2016 [26]
CUT-HP	1060	50	2017 [27]
NCU-VI Systems	850	25	2018 [28]
WUT-VI Systems	850	80	2020 [29]

rate of the NRZ-OOK transmission beyond 100 Gbit/s is setting several VCSEL chips as the VCSEL array to aggregate the whole data rate.

B. Encoding the VCSEL With the PAM-4 Data Format for Upgrading the Data Centers

To improve the spectral usage efficiency within the finite bandwidth for maximizing the encoding data rate of the directly modulated VCSELS in the data-center application, the 4-level pulse amplitude modulation (PAM-4) data format becomes one of the solutions to encode the VCSEL. Under the same modulation bandwidth of VCSEL, the PAM-4 data transmission exhibits double data rates as compared to the NRZ-OOK data transmission. Therefore, the VCSEL carrying the PAM-4 data can easily obtain the data rate beyond 100 Gbit/s. In 2011, Szczerba's group used the oxide-confined VCSEL to perform the PAM-4 transmission at 30 Gbit/s @ 200-m MMF and 25 Gbit/s @ 300-m MMF [30]. In 2013, the data rates of PAM-4 data transmission carried by the 850-nm were improved to 60 Gbit/s and 50 Gbit/s over 2-m and 50-m MMF, respectively [31]. In 2015, the 850-nm VCSEL carrying the 112-Gbit/s PAM-4 data over 200-m MMF was demonstrated by Zuo *et al.* [32]. In 2016, Castro and co-workers enhanced the data rate of the PAM-4 transmission to 50 Gbit/s in the 200-m wideband MMF case via a pre-distortion technology [33]. Szczerba *et al.* further employed the data pre-emphasis process to improve the data rate to 94 Gbit/s for the PAM-4 transmission carried by 850-nm VCSEL [34]. Finisar Corporation utilized four 45-Gbit/s VCSEL chips to demonstrate the PAM-4 data transmission with a total data rate of 180 Gbit/s over 300-m OM4 MMF [35]. VI-Systems also

used the PAM-4 data to directly modulate the SM VCSEL for achieving the 108-Gbit/s PAM-4 transmission over 100-m MMF [36]. Huawei and Keyseight Technologies reported the 112-Gbit/s PAM-4 transmission carried by the 850-nm VCSEL over 100-mm OM4 MMF for data-center interconnect [37]. In 2017, Kao and co-workers observed the transmission performance of the PAM-4 transmission carried by different-transverse-mode VCSELS [38]. The few-mode (FW) VCSEL possessed a higher throughput than SM VCSEL to exhibit the highest data rate of 52 Gbit/s for PAM-4 transmission [38]. Lavrencik *et al.* employed a pre-emphasis technology to the oxide-confined 850-nm VCSEL to further improve the data rate beyond 100 Gbit/s for the PAM-4 transmission over 100-m wideband MMF [39].

In 2018, Kao *et al.* demonstrated the PAM-4 data transmission carried by the SM VCSEL over 100-300-m OM4 MMF links [40]. In BtB and 300-m OM4 MMF conditions, the data rates of the PAM-4 transmission can be respectively obtained as 64 Gbit/s and 48 Gbit/s [40]. In 2019, Zhang and co-workers used 850-nm VCSEL to perform the PAM-4 transmission at 137 Gbit/s over the 40-cm optical backplane [41]. Sun *et al.* proposed a novel 2-dimensional (2D) soft decision method to improve the data rate of the PAM-4 transmission carried by the 850-nm VCSEL to 112 Gbit/s [42]. Moreover, the same group further added the equalization technology to perform the PAM-4 transmission at 100 Gbit/s over 100-m MMF [43]. Lavrencik's group utilized the 1060-nm VCSEL to demonstrate the PAM-4 transmission at 100 Gbit/s over 100-m OM5 MMF [44]. In 2020, the same group changed to the unpacked 850-nm VCSEL with a modulation bandwidth of 28 GHz to transmit the PAM-4 data at 168 Gbit/s over 50-m OM5 MMF [45]. Huang and co-workers compared the transmission performance of the PAM-4 transmission over OM4 and OM5 MMFs [46]. Under the pre-emphasis technology, the data rate of the PAM-4 transmission over 100-m OM5 MMF was obtained as 64 Gbit/s [46]. Huawei Technologies Co. utilized the low complexity Volterra nonlinear equalizer, PR signaling, and noise cancellation module to perform the single-lane PAM-4 transmission at 200 Gbit/s over 100-m MMF [47]. In 2021, Lo and co-workers improved the data rate of the PAM-4 data transmission to 96 Gbit/s in BtB condition and 70 Gbit/s over 100-m OM5 MMF link via the pre-emphasis technology [48]. Corning Inc. also presented the 52-Gbit/s PAM-4 data transmission carried by the SM VCSEL [49]. VI-Systems observed that the 850-nm and 910-nm SM VCSELS carried the 106-Gbit/s PAM-4 data to achieve the IEEE802.3cm standard in the future [50]. The related reports about the PAM-4 data transmission carried by the VCSEL are summarized in Fig. 2 and Table II. From the abovementioned discussion, the PAM-4 data format carried by the VCSEL can achieve a data rate beyond 100 Gbit/s for the data-center application in the future.

C. Encoding the VCSEL With the QAM-OFDM Data Format for Wireless and Mobile Communications

In addition to the data center applications, VCSELS have also been considered for bridging the wired and wireless access networks to extend the coverage of mobile communications.

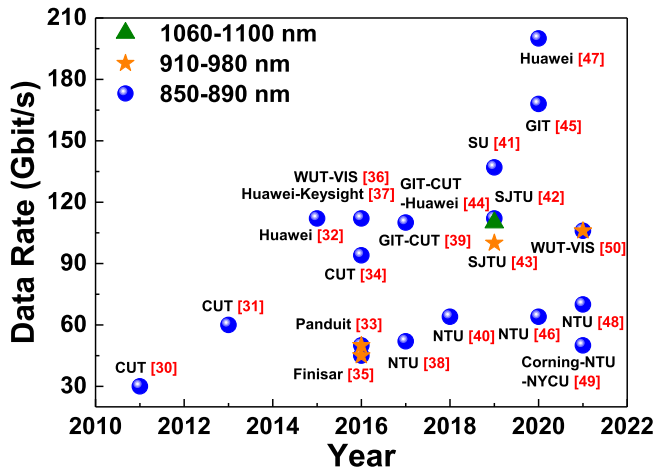


Fig. 2. The developing progress on the transmission rate of PAM-4 data format carried by the VCSEL.

TABLE II
LUMINESCENT WAVELENGTH AND BIT RATES OF THE PAM-4 TRANSMISSION CARRIED BY THE VCSEL

Group	Wavelength (nm)	Bit Rate (Gbit/s)	Year [Ref]
CUT	850	30	2011 [30]
CUT	850	60	2013 [31]
Huawei	850	112	2015 [32]
Panduit	980	50	2016 [33]
CUT	850	94	2016 [34]
Finisar	850-950 (SWDM)	45 (Single), 180 (SWDM)	2016 [35]
WUT-VI Systems	850	112	2016 [36]
Huawei-Keysight	850	112	2016 [37]
NTU	850	52	2017 [38]
GIT-CUT	850	110	2017 [39]
NTU	850	64	2018 [40]
Shanghai University (SU)	850	137	2019 [41]
Shanghai Jiao Tong University (SJTU)	850	112	2019 [42]
SJTU	980	100	2019 [43]
GIT-CUT-Huawei	1060	110	2019 [44]
GIT	850	168	2020 [45]
NTU	850	64	2020 [46]
Huawei	850	200	2020 [47]
NTU	850	70	2021 [48]
Corning-NTU-NYCU	850	54	2021 [49]
WUT-VI Systems	850	106 (850), 106 (910)	2021 [50]
WUT-VI Systems	910	106 (910)	2021 [50]

In general, the VCSEL has already emerged as a potential candidate of the front-haul optical transmitter not only for bridging between the central office and the 5th-generation mobile internet base station but also for interconnecting the distributed 5th-generation mobile internet base stations. Several industrial companies have started to provide solutions or products of the VCSEL front-haul transmitters for the 5th-generation base station equipment. Another alternative approach utilizes the VCSEL with dual-mode output as a front-haul transmitter to embed the wireless carrier on the optical carrier for the advanced radio-over-fiber networks. This method is still in the progress of laboratory study without significant industrial application in the foreseeable future. To effectively use the modulation bandwidth

of the VCSEL, the quadrature amplitude modulation orthogonal frequency division multiplexing (QAM-OFDM) data format was proposed because this data format can provide several times larger than the NRZ-OOK data format. Therefore, the data rate for this VCSEL-MMF transmission is easily achieved to 100 Gbit/s even though the modulation bandwidth of the VCSEL is below 20 GHz. Moreover, the Hermitian symmetry in digital signal processing (DSP) technology is usually employed to make the QAM-OFDM data format form the real-valued time-domain signal. This converted data format is regarded as a special case of QAM-OFDM data format and called as the discrete multitone (DMT) data. In 2007, Lee *et al.* utilized the DMT data format for directly modulating the 850-nm VCSEL to demonstrate the DMT transmission over 730-m MMF [51]. In 2009, the same group increased the transmission distance to achieve the DMT transmission at 30 Gbit/s @ 500-m MMF and 28 Gbit/s @ 1-km MMF [52]. In 2014, Olmedo and co-workers employed the carrierless amplitude phase (CAP) algorithm to directly modulate the 850-nm VCSEL with a modulation bandwidth of 10.1 GHz for achieving data rates of 70.4 Gbit/s @ 100-m OM3 MMF and 80 Gbit/s @ 1-m OM3 MMF [53]. Lu *et al.* utilized the QAM-OFDM data format with bit-loading and nonlinear compensation technologies to demonstrate the VCSEL-MMF network at 15 Gbit/s over 2-km OM4 MMF [54]. In 2015, the same group directly modulated the SM VCSEL with a modulation bandwidth of 12 GHz via the DMT data format to improve the data rate to 50 Gbit/s @ 2.2-km OM4 MMF [55]. Ling *et al.* used the same data format to perform the VCSEL-MMF link at 100 Gbit/s [56]. In 2016, Puerta *et al.* combined the OFDM data format and the bit-loading technology to perform the QAM-OFDM transmission with a data rate of 107.5 Gbit/s over 10-m MMF [57]. Meanwhile, the most significant progress achieved in the industry is that Huawei also utilized the DMT data format to present the different VCSEL-MMF links with data rates of 120 Gbit/s @ BtB case, 118 Gbit/s @ 100-m OM4 MMF, 117 Gbit/s @ 200-m OM4 MMF, and 112 Gbit/s @ 300-m OM4 MMF [58].

More interesting works on the high-speed VCSEL-based optical links with the versatile QAM-OFDM data format have successively emerged after 2017. For example, Tsai *et al.* directly modulated the 850-nm MM VCSEL with a modulation bandwidth of 14 GHz by using the QAM-OFDM data format to effectively improve the whole data rate [59]. They utilized the pre-leveling process to compensate the response throughput of the MM VCSEL in the high-frequency region for improving the data rate of the MM VCSEL-based optical link to 52 Gbit/s [59]. Moreover, Kao and co-workers also observed the different-mode VCSELs to perform the 16 QAM-OFDM transmissions over 100-m OM4 MMF [60]. For different-mode VCSELs, the FM VCSEL exhibited the best transmission performance in BtB condition to deliver the 16 QAM-OFDM data at 96 Gbit/s [60]. However, the SM VCSEL can effectively suppress the modal dispersion to achieve a data rate of 80 Gbit/s for the QAM-OFDM transmission over 100-m OM4 MMF [60]. VI-Systems further improved data rates of the DMT transmission carried by the VCSEL to 161 Gbit/s over 10-m OM4 MMF and 135 Gbit/s over 550-m OM4 MMF via the pre-equalization

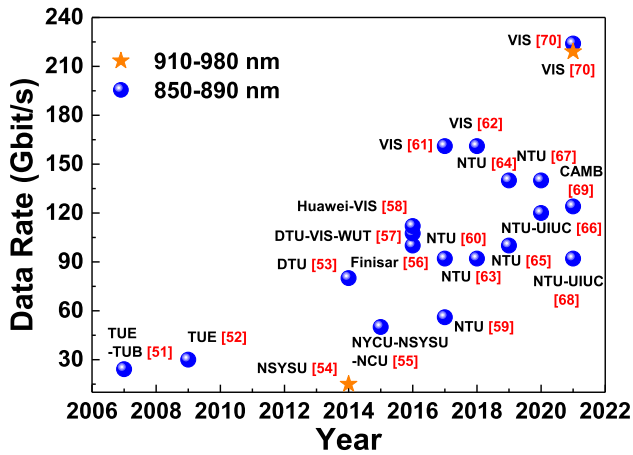


Fig. 3. The developing progress on the transmission rate of QAM-OFDM data format carried by the VCSEL.

technology [61]. In 2018, the same group achieved data rates of 135 Gbit/s @ 10-m MMF and 114 Gbit/s @ 550-m MMF under the hard-decision forward error correction (HD-FEC) limit [62]. In 2019, Kao and co-workers observed the stability of the SM VCSEL-based optical link for 1.5 hours to keep the data rate of the QAM-OFDM transmission at 96 Gbit/s [63]. Wu *et al.* demonstrated the 16 QAM-OFDM transmissions carried by the FM VCSEL at 140 Gbit/s @ BtB case and 120 Gbit/s @ 100-m OM5 MMF [64]. In 2020, Huang *et al.* controlled the VCSEL temperature and utilized the OM5 MMF as the transmission media to exhibit the 16 QAM-OFDM transmissions with the best data rate of 140 Gbit/s @ BtB case [65]–[67]. In 2021, Lin *et al.* used the photonic crystal VCSEL as a transmitter to construct the VCSEL-MMF network with a data rate of 72 Gbit/s @ 100-m OM5 MMF [68]. Bamiedakis and co-workers combined the low-complexity equalizers and the CAP data format to make the VCSEL-MMF link achieve a data rate of 124 Gbit/s @ 100-m OM4 MMF [69]. IV-Systems directly modulated 850 and 910 nm VCSELS to demonstrate the DMT transmission at 224 Gbit/s beyond IEEE802.3cm standard [70].

The related reports about the QAM-OFDM data transmission carried by the VCSEL are summarized in Fig. 3 and Table III. From the abovementioned reports, academic and industrial institutions still study how to improve the data rate from the device and data formats. Up to now, there are three main-stream data formats proposed in the VCSEL-MMF optical link, such as the on-off keying (OOK), pulsed amplitude modulation with N levels (PAM-N), and the M-ary quadrature amplitude modulation orthogonal frequency multiplexing (M-QAM OFDM) [71]. In comparison, the OOK format with the lowest spectral usage efficiency (1 bit/s/Hz) employs the simplest circuitry to demonstrate. The PAM-N format can increase the spectral usage efficiency by $\log_2 N$ within the same allowable bandwidth at a higher criterion of the signal-to-noise ratio (SNR) for error-free detection. In contrast, the M-QAM OFDM format exhibits the largest spectral usage efficiency of up to $\log_2 M$ bit/s/Hz ideally; however, the required SNR linearly increases with the $\log_2 M$. The M-QAM OFDM format also demands a more complex driving circuit with more complicated digital-analog converting

TABLE III
LUMINESCENT WAVELENGTH AND BIT RATES OF THE QAM-OFDM TRANSMISSION CARRIED BY THE VCSEL

Group	Wavelength (nm)	Bit Rate (Gbit/s)	Year [Ref]
TUE-TU Berlin	850	24.1	2007 [51]
TUE	850	30	2009 [52]
DTU	850	80	2014 [53]
NSYSU	980	15	2014 [54]
NYCU-NSYSU-NCU	850	50	2015 [55]
Finisar	850	100	2016 [56]
DTU-VI	850	107.5	2016 [57]
Systems-WUT	850	112	2016 [58]
Huawei-VI Systems	850	112	2016 [58]
NTU	850	56	2017 [59]
NTU	850	92	2017 [60]
VI Systems	850	161	2017 [61]
VI Systems	850	161	2018 [62]
NTU	850	92	2018 [63]
NTU	850	140	2019 [64]
NTU	850	100	2019 [65]
NTU-UIUC	850	120	2020 [66]
NTU	850	140	2020 [67]
NTU-UIUC	850	92	2021 [68]
Cambridge	850	124	2021 [69]
VI Systems	850	224 (850)	2021 [70]
	910	219 (910)	

devices and higher power consumption. At the current stage, the data-center network has gradually transferred its data format from the conventional OOK to the advanced PAM-4. Nevertheless, the M-QAM OFDM format will be soon considered in the next-generation data centers or the wireless base stations for the seamless coverage between optical wired and microwave wireless networks without data format transfer. For the next section, the QAM generalized frequency division multiplexing (QAM-GFDM) and bit-loaded DMT data formats to modulate the MM VCSEL are introduced in detail.

II. EXPERIMENTAL DEMONSTRATION FOR ENCODING VCSELS WITH HIGH-LEVEL QAM-OFDM FORMAT

To detail the design of the VCSEL with improved modulation bandwidth, the algorithm of the complex data format with high spectral usage efficiency, and the performance evaluation of the VCSEL under high-level complex amplitude/phase encoding, the newly designed multi-mode VCSEL device carrying the QAM-GFDM and bit-loading DMT algorithms was taken as the example device and the data format for a demonstration in this review. In particular, the achievable Baud rate for the QAM-GFDM data and data rate for the bit-loaded DMT format are declared in the following sections for realizing the transmission capability of complex data formats carried by the MM-VCSELS with high SNR beyond 18 dB and corresponding BER below the error-free criterion of 3.8×10^{-3} after performing HD-FEC. In more detail, the effect of the ambient temperature on the performance degradation of the MM VCSEL is also monitored and compared to understand the thermal stability of the MM-VCSEL when encoding with such complex data formats.

A. Design of Bi-layer-oxide Confined MM VCSEL

Fig. 4(a) exhibits the schematic diagram of the bi-layer-oxide confined MM VCSEL. For the MM VCSEL confined by the

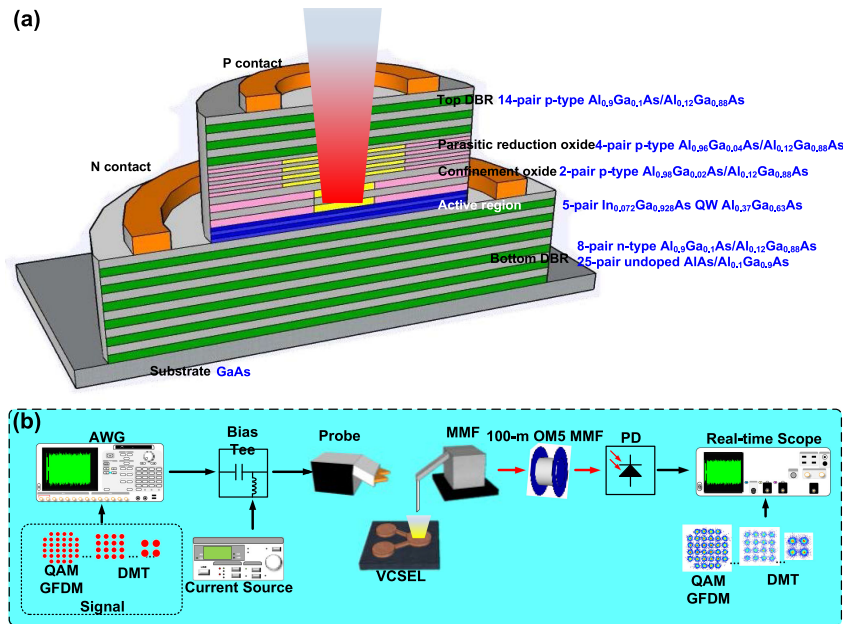


Fig. 4. (a) The schematic diagram of the MM VCSEL chip with a bi-layer oxide confined aperture, and (b) the encoding and transmission setup of the 850 nm VCSEL chip without or with 100-m OM5-MMF link.

bi-layer-oxide mesa, the 8-pair Al_{0.9}Ga_{0.1}As/Al_{0.12}Ga_{0.88}As layers and 25-pair undoped AlAs/Al_{0.1}Ga_{0.9}As layers were deposited upon a GaAs substrate to construct the bottom n-type distributed Bragg reflector (DBR) mirror. In general, enlarging the multi-quantum-well (MQW) numbers acquires not only the high optical gain and power but also the large threshold current and small modulation bandwidth. From the abovementioned discussion, the 5-pair In_{0.072}Ga_{0.928}As multi-quantum-well (MQW) active layers were designed and fabricated upon the n-DBR layer. The 2-pair Al_{0.98}Ga_{0.02}As/Al_{0.12}Ga_{0.88}As layers effectively confine the current flow. The 4-pair Al_{0.96}Ga_{0.04}As/Al_{0.12}Ga_{0.88}As layers were utilized to reduce the parasitic capacitance. Then, the bi-layer oxide region was designed within the p-type DBR layer to confine the carriers and photons. Moreover, bi-parabolic doping was utilized to obtain the flattened valence band for achieving the highly reflective resonant cavity [72]. The bi-parabolic doping technology also enhances the hole mobility to decrease the optical loss of the device [73]. The highly-doped p-type DBR layer was grown by the 14-pair Al_{0.9}Ga_{0.1}As/Al_{0.12}Ga_{0.88}As layers to improve the carrier injection efficiency. Furthermore, the p-type DBR layer can decrease the DBR resistance to suppress the heating effect [74]. On the other hand, the continuously graded molar ratio of the DBR layers was designed to decrease the interfacial potential barriers for obtaining the lower threshold current of the MM VCSEL. Furthermore, multiple Al_{0.98}Ga_{0.02}As layers were oxidized to confine the transverse mode number of the MM VCSEL. When the size of the emission aperture is decreased to reduce the transverse mode numbers, the differential resistance of the MM VCSEL concurrently enlarges to decay the differential quantum efficiency. This phenomenon effectively increases the power consumption and degrades the SNR after data encoding [75]. The small oxide aperture for the MM VCSEL exhibits a short lifetime and large heat accumulation to decay the modulation performance [76]. Therefore, the suitable

design for the oxide aperture of MM VCSEL can optimize the modulation bandwidth and spectral linewidth of the device. In addition, the ground-signal (GS) coplanar electrodes were used for decreasing the parasitic capacitance and suppressing the VCSEL size. The thin benzocyclobutene (BCB) passivation layer with a low dielectric constant was fabricated to suppress the charging/discharging time of the device for enhancing the modulation speed.

B. Algorithms and Transmission Platform for MM VCSELs Carrying the QAM-GFDM and Bit-Load DMT Data Over 100-m OM5-MMF Link

Fig. 4(b) exhibits the experimental setup of the QAM-GFDM and bit-load DMT data carried by the MM VCSEL with/without 100-m OM5 MMF link. The electrical 32-QAM GFDM and bit-loaded DMT data streams were produced from the homemade MATLAB program and generated by an arbitrary waveform generator (AWG) with a modulation bandwidth of 45 GHz, a sampling rate of 120 GS/s, and a modulation amplitude of 800 mV to modulate the MM VCSEL. The DC bias and 32-QAM GFDM/bit-load DMT data stream were combined via a 65-GHz bias-tee to form the mixed signal. To drive the MM VCSEL, a 67-GHz GS coplanar probe was utilized to send into the device. To observe the transmission performance for the MM VCSEL operated at different temperatures, the MM VCSEL chip was placed on the thermoelectric (TE) cooler with a water-cooling system. The optical 32-QAM GFDM and bit-loaded DMT data streams were received by the lensed OM5 MMF and passed through the 100-m OM5 MMF link. In general, the OM5 MMF exhibits lower intensity degradation and phase variation to demonstrate a better transmission performance as compared to OM4 MMF. After passing through the 100-m OM5 MMF link, the received data streams delivered by the MM VCSEL were collected by a high-speed photodetector to perform the

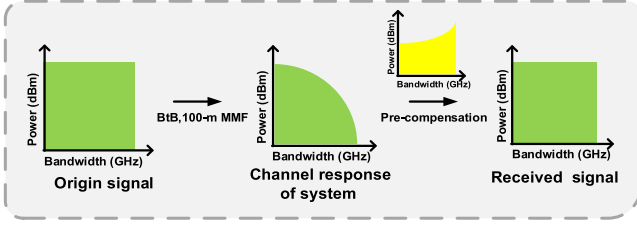


Fig. 5. The synopsis of the pre-emphasis technique.

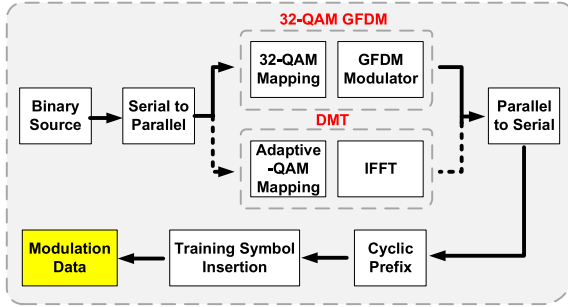


Fig. 6. The block diagram of 32-QAM GFDM and DMT data generation.

optical-to-electrical conversion. To examine the received data formats, the 32-QAM GFDM and bit-loaded DMT data formats were resampled by a real-time oscilloscope with a sampling rate of 200 GS/s and an analog bandwidth of 70 GHz. Finally, the EVM, SNR, and BER performances of the 32-QAM GFDM and bit-loaded DMT data were obtained by the homemade MATLAB program. For broadband QAM-GFDM data transmission, the pre-emphasis process was applied for compensating the waveform distortion. Before implementing the pre-emphasis, broadband OFDM data was employed to encode the MM VCSEL. After passing through the OM5 MMF, the channel response can be obtained by examining the training sequence of the received OFDM data. Therefore, the intensity and phase information of the entire transmission system is also acquired. According to the examined channel response of the whole transmission system, the pre-emphasis process implements energy and phase redistribution to pre-compensate the degraded SNR spectra of 32-QAM GFDM data at the transmitting end. The peak-to-peak amplitude of the pre-emphasized data is somewhat suppressed because of the energy redistribution as the power consumption at different bands depends on the deterioration of the channel response, as shown in Fig. 5. In contrast, the bit-loading DMT algorithm does not apply the pre-emphasis technology in our case.

III. RESULT AND DISCUSSION

A. The Algorithms for Synthesizing 32-QAM GFDM and Bit-Loaded DMT Data Formats

To explore the encoding capability and transmission performance of the MM VCSEL directly modulated by the complex data formats demanding relatively high SNR and BER under HD-FEC, the block diagrams of different algorithms for synthesizing the 32-QAM GFDM and the bit-loaded DMT data formats are depicted in Fig. 6. First of all, a pseudorandom binary sequence (PRBS) with a bit length of $2^{15}-1$ was generated

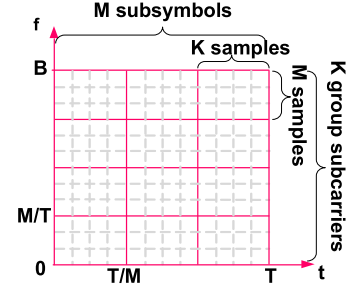


Fig. 7. Time-frequency transformation matrix of GFDM algorithm.

from the AWG. After serial-to-parallel conversion, the PRBS was mapped onto 32-QAM constellation points and utilized via a GFDM modulator to generate the 32-QAM GFDM waveform in the time domain. On the other hand, the DMT waveform in the time domain was obtained by arranging the PRBS with the bit-loading-based adaptive QAM mapping and implementing inverse fast Fourier transform (IFFT). As a result, each subcarrier can be arranged to the appropriate QAM level according to the analysis of SNR performance. After the IFFT with a matrix length of 512, a real-valued waveform in the time domain would be obtained by arranging the subcarrier of DMT and GFDM in the frequency domain. In comparison with DMT and traditional OFDM data, the GFDM data format utilizes the GFDM modulator containing pulse shaping, circular convolution, FFT, and IFFT processes in the time-frequency transformation matrix instead of the traditional IFFT operation in bit-load DMT and OFDM data formats [77], [78]. Also, the Cyclic Prefix (CP) ratio with a value of $1/256$ is added to mitigate the effect of the inter symbol interference (ISI) and the inter-carrier interference (ICI) after transmission for 32-QAM GFDM and bit-loaded DMT formats.

In comparison with other data formats, the key advantage of GFDM is the suppression of the OOB emission to avoid mutual interference of OFDM subcarriers in the frequency domain and the reduction of the peak-to-average power ratio (PAPR) to improve the nonlinear distortion and clipping effect caused by nonlinear electronic components. Then, the training symbols (TSs) used in the 32-QAM GFDM and bit-loaded DMT waveforms to identify the beginning point between continuous data streams would be removed at the receiving end for correct demodulation. The time-frequency transformation matrix for QAM GFDM data is shown in Fig. 7. GFDM data format combines OFDM format and single-carrier frequency domain equalization (SC-FDE) to rearrange OFDM subcarriers. The N OFDM subcarriers are reallocated into K GFDM group subcarriers and M GFDM subsymbols in a redefined matrix by following a rule of $N = K \times M$. When the K is equal to N in the extreme case, the time-frequency transformation matrix of GFDM can be turned into OFDM. In addition, the time-frequency transformation matrix of GFDM can be changed to SC-FDE as the M is equal to N [79].

B. Transmission Performance of the MM VCSEL Encoded With 32-QAM GFDM Data Stream

When the GFDM algorithm has to obey the rule of $N = K \times M$ with N total subcarriers, K as the GFDM group subcarriers

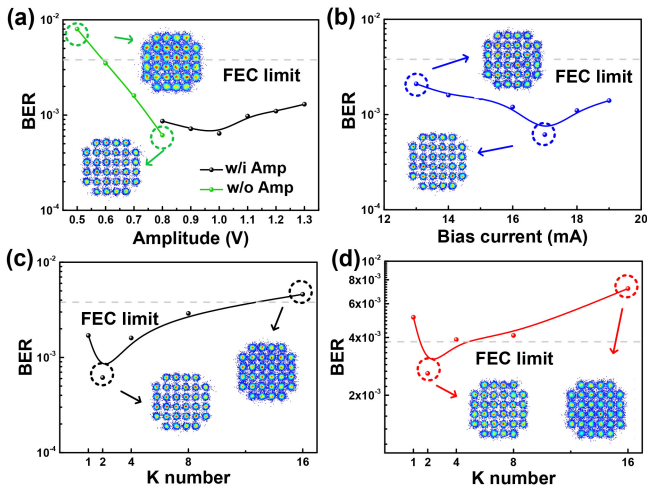


Fig. 8. The (a) BER versus peak amplitude and (b) BER versus DC bias for the 32-QAM GFDM data with the K number of 2 carried by the MM VCSEL. The BERs of 32-QAM GFDM data with different K numbers in the (c) BtB and (d) 100-m OM5 MMF cases.

can be set as 2^n with n denoting the integer [79]. In our case, there are 96 subcarriers totally to be divided from $K = 1$ to $K = 16$ groups such that subsymbols can be allocated from 96 to 6 within one group. Fig. 8 exhibits the transmission performances of the 32-QAM GFDM data modulated by the MM VCSEL at a modulation bandwidth of 22.5 GHz. In this work, 96 subcarriers share the encodable bandwidth of 22.5 GHz for delivering the GFDM data stream. By raising the peak amplitude of the GFDM data from 0.5 to 0.8 V, the received GFDM data stream with the K number of 2 exhibits its average SNR increasing from 17.2 dB to 20 dB, error vector magnitude (EVM) decreasing from 13.81% to 10%, and BER improving from 8×10^{-3} to 6.15×10^{-4} , as shown in Fig. 8(a). Owing to the maximal output peak-to-peak voltage (V_{pp}) of only 0.8 V from the AWG, the boost amplifier is used to increase the peak amplitude of the GFDM data. However, using the boost amplifier induces the power saturation and additional noise to degrade the BER performance under the higher V_{pp} condition. Fig. 7(b) shows that increasing the DC bias from 13 ($13I_{th}$) to 17 mA ($17I_{th}$) effectively suppresses the relative intensity noise of the MM VCSEL to optimize the receiving BER of the 32-QAM GFDM data from 2.1×10^{-3} to 6.2×10^{-4} with an average SNR enhancing from 18.6 dB to 20 dB and an EVM improving from 11.4% to 10%. However, the operated DC bias further enlarges beyond 19 mA to cause the BER degradation to 2.1×10^{-3} with decreased SNR of 19.2 dB and increased EVM of 10.9%. That is because the output power of the GFDM data saturates to induce the waveform clipping and the data waveform distortion when the MM VCSEL is operated at the higher DC bias.

The BERs of the 32-QAM GFDM data with different K numbers delivered by the MM VCSEL in the BtB case are shown in Fig. 8(c). By selecting the K number at 2, the best transmission performance of the 32-QAM GFDM data in the BtB case can be obtained the lowest receiving BER of 6.2×10^{-4} . In general, the better out-of-band (OOB) suppression ratio of the 32-QAM GFDM data with low K numbers can be observed.

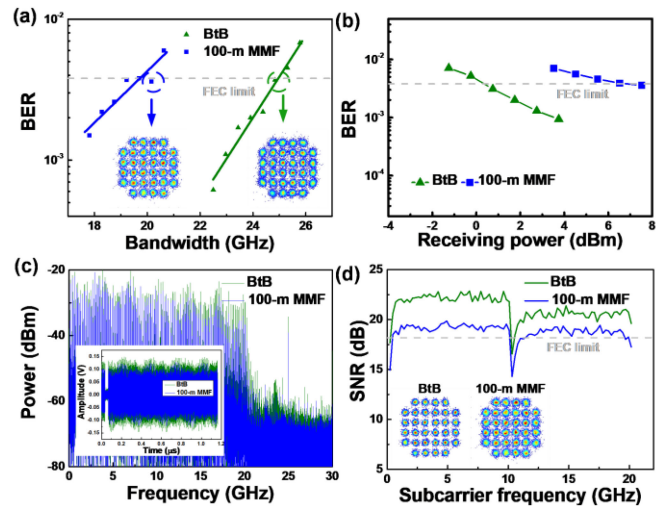


Fig. 9. (a) The BERs of the 32-QAM GFDM data carried by the MM VCSEL under different modulation bandwidths in the BtB and 100-m OM5 MMF cases. (b) The receiving power of the 32-QAM GFDM data at 101 Gbit/s delivered by the MM VCSEL in the BtB and 100-m OM5 MMF cases. The (c) RF spectra and time-domain waveforms with its (d) corresponding constellation plots and subcarrier SNR spectra for the 32-QAM GFDM transmission at 101 Gbit/s in the BtB and 100-m OM5 MMF cases.

In addition, the severer main-lobe ripple would concurrently occur. Therefore, the selection of the K numbers can optimize the transmission performance between the side-lobe attenuation and the main-lobe fluctuation. This effect is known as the ‘‘Gibb’s phenomenon’’ [80]. When the K number enlarges from 2 to 16, the ISI between two adjacent GFDM subcarriers may increase to enlarge the data degradation. After passing through 100-m OM5 MMF, the lowest BER of the 32-QAM GFDM data with the K number of 2 is also obtained as 2.6×10^{-3} , as shown in Fig. 8(d).

Furthermore, the encoding bandwidth of the 32-QAM GFDM data stream by performing the pre-emphasis process can be detuned to maximize the allowable data capacity in the BtB and 100-m OM5-MMF cases. The receiving BERs of the 32-QAM GFDM data carried by the MM VCSEL under different modulation bandwidths are displayed in Fig. 9(a). In Fig. 9(a), the average SNR of the 32-QAM GFDM data in the BtB case is degraded from 20 dB to 17.4 dB with a corresponding BER increasing from 6.15×10^{-4} to 6.8×10^{-3} when the modulation bandwidth enlarges from 22.5 GHz to 25.8 GHz. According to the HD-FEC criterion with a corresponding BER of 3.8×10^{-3} [81], the maximal modulation bandwidth of MM VCSEL can achieve 24.8 GHz for the 32-QAM GFDM data transmission with a data rate of 124 Gbit/s in the BtB case. After propagating through the 100-m OM5 MMF, the maximal modulation bandwidth would slightly decrease to 20.2 GHz with the total data rate of 101 Gbit/s because of the propagation loss and the modal dispersion. The penalty of the allowable modulation bandwidth is obtained as 4.6 GHz with the corresponding variation of the data rate at 23 Gbit/s between BtB and 100-m OM5-MMF cases.

Fig. 9(b) compares the BER versus the receiving power of the MM VCSEL carrying the 101-Gbit/s 32-QAM GFDM data

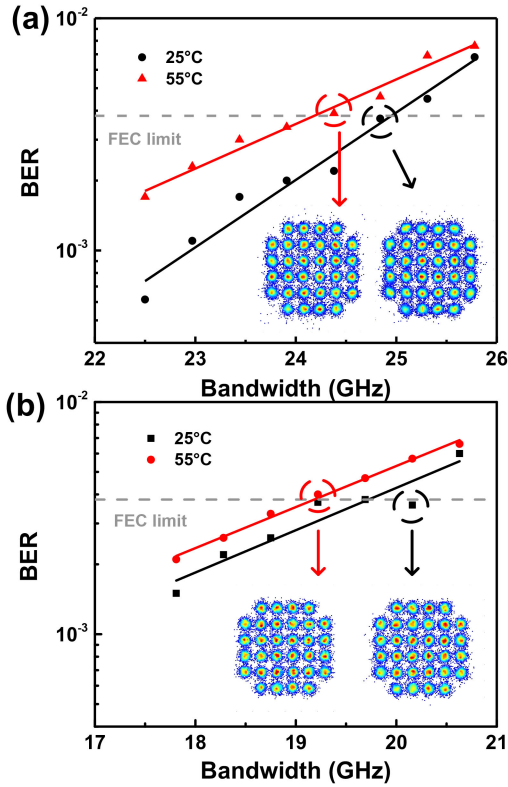


Fig. 10. The BERs and constellation plots of the 32-QAM GFDM data carried by the MM VCSEL under different modulation bandwidths in the (a) BtB and (b) 100-m OM5 MMF cases at 25 °C and 55 °C.

stream in the BtB and 100-m OM5-MMF cases. In the error-free condition, the receiving powers for the 101-Gbit/s 32-QAM GFDM data stream are obtained as 0.4 dBm in the BtB case and 6.9 dBm in the 100-m OM5 MMF case to result in a large power penalty of 6.5 dB owing to the severe modal dispersion to distort its waveform for the MM VCSEL. Fig. 9(c) shows the time-domain waveforms and RF spectra of the 101-Gbit/s 32-QAM GFDM data stream carried by the MM VCSEL in the BtB and 100-m OM5 MMF cases. Because of the power fading effect appearing during the OM5 MMF transmission, the V_{pp} of the received 101-Gbit/s 32-QAM GFDM data is decreased from 0.32 V to 0.21 V. Fig. 9(d) plots the decoded SNR spectra of the 32-QAM GFDM data with the K number of 2 in the BtB and 100-m OM5 MMF cases. Apparently, the severe modal dispersion and propagation losses during OM5-MMF transmission contribute to the blurred constellation plot of the received 101-Gbit/s 32-QAM GFDM data. Therefore, the 101-Gbit/s 32-QAM GFDM data in the 100-m OM5 MMF case exhibits its enlarged EVM from 9.4% to 12.2%, decreased average SNR from 20.5 to 18.3 dB, and degraded BER from 3.2×10^{-4} to 3.6×10^{-3} .

To characterize the thermal stability of the MM VCSEL under the long-term heating operation above 2 hrs, Fig. 10(a) exhibits the BtB transmission performance of 32-QAM GFDM carried by the MM VCSEL operated at 25 °C and 55 °C. From the previous discussion in Fig. 9(a), the maximal transmission capacity of the 32-QAM GFDM data delivered by the MM VCSEL operated

at 25 °C in the BtB case can reach 24.8 GHz (124 Gbit/s). When the temperature of the MM VCSEL increases to 55 °C, the maximal allowable data rate is slightly reduced to 23.9 GHz (119.5 Gbit/s) because the radiative recombination in the MM VCSEL decreases under high-temperature operation to reduce the output power. Moreover, Fig. 10(b) shows the BERs of the 32-QAM GFDM data under different modulation bandwidths in the 100-m OM5-MMF case when the MM VCSEL is operated at 25 °C and 55 °C. In the 100-m OM5-MMF case, the maximal transmission capacities of the 32-QAM GFDM data delivered by the MM VCSEL are obtained as 20.2 GHz (101 Gbit/s) at 25 °C and 18.8 GHz (93.8 Gbit/s) at 55 °C.

C. Transmission Performance of the MM VCSEL Encoded With Bit-loaded DMT Data

To compare with the broadband 32-QAM GFDA algorithm, the bit-loaded DMT employs the adaptive bit-loading algorithm to achieve maximal spectral-usage efficiency for improving the data capacity. Additionally, the DMT format is utilized to appropriate QAM-level mapping according to the transmission characteristics for each subcarrier. During the data transmission analysis in a certain time slot, the SNR curve is an average value of all receded and decoded bits in the QAM data stream carried by each GFDM subcarrier, which somewhat fluctuates with unexpected SNR dips occasionally occurring and disappearing by the environmental parameter perturbation. The spectral usage is dynamically adjusted for better optimizing the bit-loading DMT performance. Fig. 11(a) shows the SNR spectra of the bit-loaded DMT data carried by the MM VCSEL operated at 25 °C and 55 °C in the BtB case. When the MM-VCSEL is operated at 25 °C, the 32-QAM DMT is adopted within 19.2-GHz bandwidth to pass the HD-FEC required SNR criterion of 18.2 dB. The 16-QAM DMT is used for the band located between 19.2 GHz and 23.9 GHz with corresponding SNR ranged between 18.2 dB and 15.2 dB. The 8-QAM DMT format is selected for the band located between 23.9 GHz and 28.6 GHz. The 4-QAM DMT is employed for the bands located between 28.6 GHz and 36.1 GHz, and the BPSK format is used for DMT subcarriers beyond 36.1 GHz.

The bandwidth-dependent subcarrier numbers applied to different QAM levels are illustrated in Fig 11(b). According to the SNR spectra, the SNR sharply drops as the frequency increases. This phenomenon decreases the utilization of the QAM-level to pass the HD-FEC criterion. By setting the homemade MATLAB program with the sampling rate (s_a) of 120 GS/s, FFT size (S_{FFT}) of 512, and subcarrier numbers (N_{MQAM}) allocated in M -QAMs, the raw data rate of the bit-loaded DMT directly modulated by the MM VCSEL can be substantially achieved to 145 Gbit/s in the BtB case by using the formula of $s_a \times (N_{MQAM} \times \log_2(M))/S_{FFT}$ [79]. However, increasing the operating temperature degrades the whole bandwidth to further decay the transmission data rate. By operating the MM VCSEL at 55 °C, the bit-loaded bandwidth for the 32-QAM DMT format is suppressed to 15 GHz. For 16-QAM/8-QAM/4-QAM/BPSK, the allowable bit-loaded bandwidths are selected as 15-20.2 GHz, 20.2-27.2 GHz, 27.2-31.2 GHz, and >31.2 GHz, respectively.

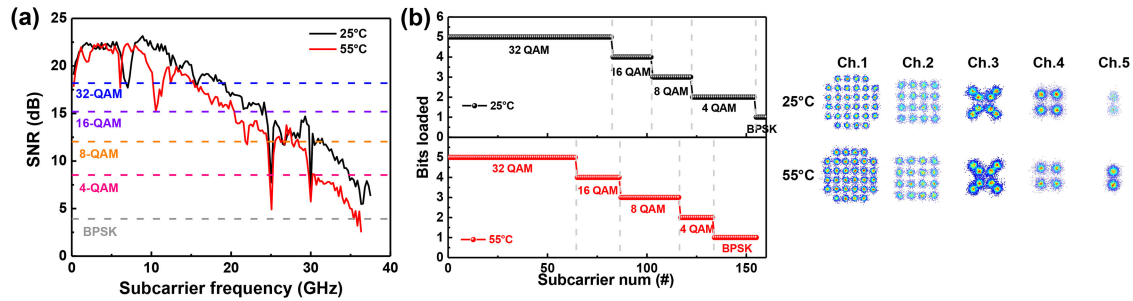


Fig. 11. The (a) received SNR spectra, (b) the bits allocation, and corresponding constellation plots of the bit-loaded DMT data transmission delivered by the MM VCSEL operated at 25 °C and 55 °C under BtB transmission.

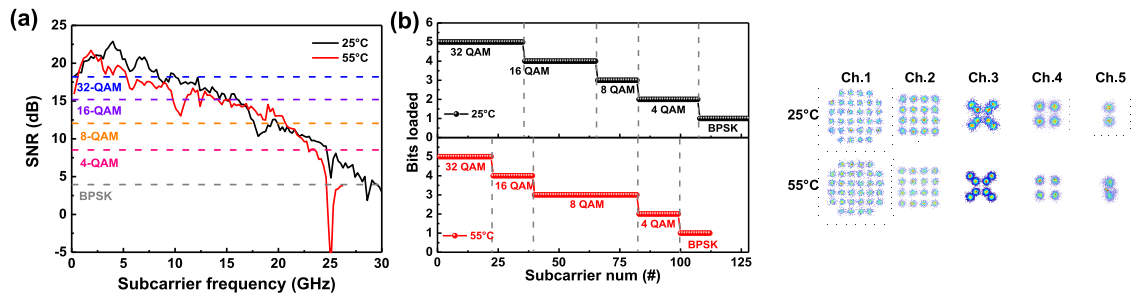


Fig. 12. The (a) received SNR spectra, (b) the bits allocation, and corresponding constellation plots of the bit-loaded DMT data transmission delivered by the MM VCSEL operated at 25 °C and 55 °C under 100-m OM5-MMF transmission.

Even if the MM VCSEL is affected by the thermal effect, the data rate can be maintained at a high speed of 130 Gbit/s.

In addition, the power degradation and modal dispersion bring out the severer SNR degradation for the bit-loaded DMT data transmission in the 100-m OM5-MMF case as compared to that in the BtB case, as shown in Figs. 12(a) and 12(b). When the MM VCSEL is operated at 25 °C, the allowable subcarrier numbers are respectively set as 35/30/17/25/21 for individually mapping the 32-QAM/16-QAM/8-QAM/4-QAM/BPSK data streams. For 32-QAM/16-QAM/8-QAM/4-QAM/BPSK, these setting subcarrier numbers can provide the respectively allowable bit-loaded bandwidths of 8.2 GHz/7 GHz/4 GHz/5.8 GHz/5 GHz to perform the bit-loaded DMT data transmission. As a result, the receiving SNRs of the bit-loaded DMT data are respectively obtained as 19.6 dB/16.4 dB/12.3 dB/9.2 dB/4.6 dB for 16-QAM/8-QAM/4-QAM/BPSK to support the total allowable data rate of 98 Gbit/s. In addition, the modulation bandwidth for the 32-QAM/16-QAM/8-QAM/4-QAM/BPSK during the bit-loaded DMT transmission carried by the MM VCSEL at 55 °C in the 100-m OM5 MMF case can be respectively decreased to 5.2 GHz/4 GHz/10 GHz/4 GHz/3 GHz with corresponding subcarriers of 22/17/43/17/13 to obtain the SNRs of 18.9 dB/16.9 dB/14.2 dB/10.2 dB/4 dB. The degraded transmission performance at 55 °C in the 100-m OM5 MMF case is attributed to the lower output of the MM VCSEL under high-temperature operation and the power fading and modal dispersion during the 100-m OM5 MMF transmission. At last, the bit-loaded DMT data transmission carried by the MM VCSEL at 55 °C in the 100-m OM5 MMF case exhibits its allowable data rate of 83 Gbit/s.

As discussed previously for the GFDM encoding on MM VCSEL operated at 25 °C, the data rate could respectively reach

TABLE IV
THE BASIC CHARACTERISTICS AND TRANSMISSION RESULTS COMPARISON OF MM VCSEL OPERATED AT 25 °C AND 55 °C

Condition	25°C	55°C
Power to Current slope	0.39 W/A	0.35 W/A
Differential resistance @17 mA	45.3 Ω	48.3 Ω
RMS spectral line width @17 mA	0.996 nm	0.953 nm
Frequency response @17 mA	23.8 GHz	20.6 GHz
32-QAM GFDM @BtB	124 Gbit/s	119.5 Gbit/s
32-QAM GFDM @100-m OM5-MMF	101 Gbit/s	93.8 Gbit/s
Bit-loading DMT @BtB	145 Gbit/s	130 Gbit/s
Bit-loading DMT @100-m OM5-MMF	98 Gbit/s	83 Gbit/s

124 Gbit/s and 101 Gbit/s before and after 100-m OM5 MMF transmission. By employing the bit-loaded DMT data format carried by the MM VCSEL operated at 25 °C, the data rate would boost to 145 Gbit/s. However, the data rate would decrease to 98 Gbit/s for 100-m OM5 MMF transmission because of the modal dispersion. The basic characteristics and transmission results of MM VCSEL operated at 25 °C and 55 °C are summarized in Table IV. For the MM VCSEL operated at 25 °C, the higher P-I slope of 0.39 W/A and frequency response of 23.8 GHz can be measured. By increasing the device temperature to 55 °C, better differential resistance and RMS spectral linewidth would be obtained. For the GFDM data transmitted by the MM VCSEL at 55 °C, the data rate will slightly drop to 120 Gbit/s in the BtB case and 94 Gbit/s in the 100-m OM5 MMF case. While directly modulated bit-loading DMT on VCSEL at 55 °C, the data rate could respectively achieve 130 Gbit/s and 83 Gbit/s for the BtB and 100-m OM5 MMF transmission.

By summarizing all the transmission results reported from previous works by different research groups to date, the achieved data rate versus year shown in Fig. 13 reveals the historical

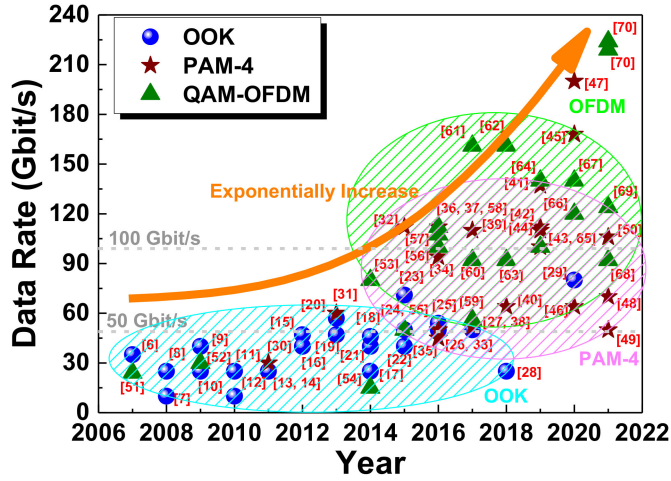


Fig. 13. The developing progress on the transmission data rate with multiple formats carried by the VCSEL.

progress and developing trend on the multiple-format transmission carried by the VCSEL. Obviously, the allowable data rate of the VCSEL-MMF link is exponentially increased year by year because the increasing demand for high-speed and high-capacity networks urges the fast-developing progress of the VCSELS in recent years. From different circles plotted in Fig. 12 to represent the different data formats, the NRZ-OOK data can only catch up the pace of the transmission standard for the data center applications with a data rate of 50 Gbit/s per channel, such as the IEEE802.3bs and the 400GBASE-SR8 defined in the IEEE 802.3cm. However, the ultimate encoding data rate for the NRZ-OOK data transmission carried by the single VCSEL is still hard to achieve 100 Gbit/s per single channel owing to the inherent limitation set by VCSELS.

In view of the developing progress on high-speed VCSELS, the direct modulation bandwidth of the VCSEL is inherently limited by its emission aperture size which determines the charging/discharging time constant, and the error-free transmission further relies on the suppression or compensation of modal compensation caused by multimode fiber. Currently, the developing trend is mainly focused on employing metallic doping in the distributed Bragg reflector for reducing the resistance of the VCSEL to shorten the switching response for broadening the modulation bandwidth. In the meantime, the shrinkage of the emission aperture size and metallic diffusion area is designed to obtain single-mode lasing for suppressing the modal dispersion in multimode fiber. Nevertheless, the VCSEL with a smaller aperture also emits a lower power such that the modulation throughput is decreased to degrade the SNR ratio in general. Toward beyond 100-Gbit/s transmission with the data format of low complexity, the design of a quasi-single-mode VCSEL is therefore considered as the potential candidate to compromise between the modal dispersion and the modulation throughput. Alternatively, the few-mode VCSEL encoded by complex data formats with high spectral-usage-efficiency is the best way to elevate the total transmission data rate within the same allowable

bandwidth. For achieving the 400-Gbit/s, 800-Gbit/s, and 1.6-Tbit/s transmission or even beyond, the data rate is necessary to achieve above 100 Gbit/s per single VCSEL for reducing the channel number toward mandatory purposes including the reduced power consumption and the efficient heat dissipation. This development effectively decreases the whole volume and cost of the multi-lane VCSEL transmitter module designed for future data centers. Therefore, the higher leveled PAM-4 or even the more complex QAM-OFDM data formats have been gradually introduced to encode the VCSELS for transmission capability elevation owing to their more important roles played in the future. No matter what data format is used to fit the versatile communication networks in the future, the VCSEL-MMF links are still the most important component to construct the short-reach intra-data-center application.

IV. CONCLUSION

The developing progress on the structural design and data algorithms to enable the VCSELS for transmitting multiple complex data formats beyond 100-Gbit/s has been reviewed in this paper. Up to now, academic and industrial institutions still keep their research pace on studying how to improve the allowable data rate of various data formats carried by the VCSEL device. Persistent efforts are endeavored not only to achieve the IEEE802.3 standards for data center applications but also to initiate the new era of wired and wireless network coverage. To date, the highest allowable data rates of the single-VCSEL-based optical link for transmitting the NRZ-OOK format at 80 Gbit/s in the BtB case, the PAM-4 format at 168 Gbit/s over 150-m OM5 MMF, and the QAM-OFDM format at 224 Gbit/s in the BtB case have been achieved in 2021. For the high-level complex data-format transmission with rigorous demand of the SNR, this work demonstrates the most up-to-date 32-QAM GFDM data algorithm with optimized amplitude and K value for encoding the MM VCSEL. By modulating the MM VCSEL operated at a DC bias of 17 mA with a peak-to-peak amplitude of the GFDM data at 800 mV, the EVM, SNR, and BER of the receiving 32-QAM GFDM data can be respectively improved to 10%, 20 dB, and 6.15×10^{-4} by setting the K number of 2. Such a $K = 2$ condition is verified as a compromise between the main-lobe fluctuation and side-lobe attenuation of the 32-QAM GFDM data spectrum observed in the frequency domain. Under the proposed parametric optimization in this work, the typical MM VCSEL can successfully deliver the 32-QAM GFDM data stream with a maximal transmission capacity of 124 bit/s in the BtB case. For short-reach applications, the 32-QAM GFDM (with $K = 2$) data transmission after 100-m OM5 MMF link is also demonstrated with an allowable data rate of 101 Gbit/s after optimization to provide the power penalty of 6.5 dB because of the SNR degradation caused by fiber loss and modal dispersion. To achieve higher spectral-usage efficiency for maximal transmission data rate, the bit-loaded DMT technique is implemented by rearranging each subcarrier to the appropriate QAM-level according to the SNR spectrum. In this way, the data rate of the bit-loaded DMT data will be promoted to 145 Gbit/s in the BtB case. However, the bit-loaded DMT data in the 100-m OM5

MMF case exhibits its allowable data rate of 98 Gbit/s because of modal dispersion and power degradation. Moreover, to analyze the thermal stability of MM VCSEL, the basic characteristics and transmission performance of the MM VCSEL operated at 25 °C and 55 °C are compared. As the device temperature enlarges to 55 °C, the maximal output power would decrease and easily reach the roll-off effect. At the same time, the dP/dI fluctuation indicates the signal deterioration. By utilizing 32-QAM GFDM and bit-loading DMT, the maximal data rate in BtB case could respectively achieve 119.5 Gbit/s and 130 Gbit/s when operating the MM VCSEL at 55 °C. After propagating through OM5 MM fiber (MMF), the transmission capacity of the VCSEL operated at 55 °C would decrease to 93.8 Gbit/s for 32-QAM GFDM and 83 Gbit/s for bit-loading DMT owing to the modal dispersion in OM5 MMF. With illustrating the comparison on the allowable data rate for the VCSELs with encoding different complex data formats, this review declares the future developing trend for the directly modulated VCSEL transmitters toward the beyond-100Gbit/s operation in different applications.

REFERENCES

- [1] IEEE P802.3bs, "200 Gb/s and 400 Gb/s Ethernet Task Force," 2018. [Online]. Available: <http://www.ieee802.org/3/bs/>
- [2] IEEE P802.3cm, "400 Gb/s over Multimode Fiber Task Force," [Online]. Available: <http://www.ieee802.org/3/cm/>
- [3] 40G-SWDM4 MSA technical specifications Rev 2, SWDM multisource agreement, Nov. 2017.
- [4] 100G-SWDM4 MSA Technical Specifications Rev 2, SWDM Multisource agreement, Nov. 2017.
- [5] Ethernet roadmap, Accessed: Nov. 2018. [Online]. Available: <https://ethernetalliance.org/the-2018-ethernet-roadmap/>
- [6] Y.-C. Chang, C. S. Wang, and L. A. Coldren, "High-efficiency, high-speed VCSELs with 35 Gbit/s error-free operation," *Electron. Lett.*, vol. 43, no. 19, pp. 1022–1023, Sep. 2007.
- [7] J.-W. Shi, C.-C. Chen, Y.-S. Wu, S.-H. Guol, C. Kuo, and Y.-J. Yang, "High-power and high-speed Zn-diffusion single fundamental-mode vertical-cavity surface-emitting lasers at 850-nm wavelength," *IEEE Photon. Technol. Lett.*, vol. 20, no. 13, pp. 1121–1123, Jul. 2008.
- [8] P. Westbergh, J. S. Gustavsson, A. Haglund, H. Sunnerud, and A. Larsson, "Large aperture 850 nm VCSELs operating at bit rates up to 25 Gbit/s," *Electron. Lett.*, vol. 44, no. 15, pp. 907–908, Jul. 2008.
- [9] S. A. Blokhin *et al.*, "Oxide-confined 850 nm VCSELs operating at bit rates up to 40 Gbit/s," *Electron. Lett.*, vol. 45, no. 10, pp. 501–503, May 2009.
- [10] H. Hatakeyama *et al.*, "25 Gbit/s 100 °C operation of highly reliable InGaAs/GaAsP-VCSELs," *Electron. Lett.*, vol. 45, no. 1, pp. 45–46, Jan. 2009.
- [11] C. Chen, Z. Tian, K. D. Choquette, and D. V. Plant, "25-Gb/s direct modulation of implant confined holey vertical-cavity surface-emitting lasers," *IEEE Photon. Technol. Lett.*, vol. 22, no. 7, pp. 465–467, Apr. 2010.
- [12] B. Zhu, T. F. Taunay, M. F. Yan, M. Fishteyn, G. Oulundsen, and D. Vaidya, "70-Gb/s multicore multimode fiber transmissions for optical data links," *IEEE Photon. Technol. Lett.*, vol. 22, no. 22, pp. 1647–1649, Nov. 2010.
- [13] P. Moser *et al.*, "81 fJ/bit energy-to-data ratio of 850 nm vertical-cavity surface-emitting lasers for optical interconnects," *Appl. Phys. Lett.*, vol. 98, no. 23, Jun. 2011, Art. no. 231106.
- [14] G. Fiol, J. A. Lott, N. N. Ledentsov, and D. Bimberg, "Multimode optical fibre communication at 25 Gbit/s over 300 m with small spectral-width 850 nm VCSELs," *Electron. Lett.*, vol. 47, no. 14, pp. 810–811, Jul. 2011.
- [15] P. Westbergh *et al.*, "High-speed 850 nm VCSELs with 28 GHz modulation bandwidth operating error-free up to 44 Gbit/s," *Electron. Lett.*, vol. 48, no. 18, pp. 1145–1147, Aug. 2012.
- [16] J. A. Lott, A. S. Payusov, S. A. Blokhin, P. Moser, N. N. Ledentsov, and D. Bimberg, "Arrays of 850 nm photodiodes and vertical cavity surface emitting lasers for 25 to 40 Gbit/s optical interconnects," *Phys. Status Solidi C*, vol. 9, no. 2, pp. 290–293, Jan. 2012.
- [17] R. Safaisini, E. Haglund, P. Westbergh, J. S. Gustavsson, and A. Larsson, "20 Gbit/s data transmission over 2 km multimode fibre using 850 nm mode filter VCSEL," *Electron. Lett.*, vol. 50, no. 1, pp. 40–42, Jan. 2014.
- [18] P. Moser, J. A. Lott, P. Wolf, G. Larisch, H. Li, and D. Bimberg, "Error-free 46 Gbit/s operation of oxide-confined 980 nm VCSELs at 85 °C," *Electron. Lett.*, vol. 50, no. 19, pp. 1369–1071, Sep. 2014.
- [19] P. Westbergh *et al.*, "High-speed oxide confined 850-nm VCSELs operating error-free at 40 Gb/s up to 85 °C," *IEEE Photon. Technol. Lett.*, vol. 25, no. 8, pp. 768–771, Apr. 2013.
- [20] P. Westbergh, E. P. Haglund, E. Haglund, R. Safaisini, J. S. Gustavsson, and A. Larsson, "High-speed 850 nm VCSELs operating error free up to 57 Gbit/s," *Electron. Lett.*, vol. 49, no. 16, pp. 1021–1023, Aug. 2013.
- [21] F. Tan, M.-K. Wu, M. Liu, M. Feng, and N. Holonyak, "850 nm oxide-VCSEL with low relative intensity noise and 40 Gb/s error free data transmission," *IEEE Photon. Technol. Lett.*, vol. 26, no. 3, pp. 289–292, Feb. 2014.
- [22] P. Westbergh, J. S. Gustavsson, and A. Larsson, "VCSEL arrays for multicore fiber interconnects with an aggregate capacity of 240 Gb/s," *IEEE Photon. Technol. Lett.*, vol. 27, no. 3, pp. 296–299, Feb. 2015.
- [23] D. M. Kuchta *et al.*, "A 71-Gb/s NRZ modulated 850-nm VCSEL-based optical link," *IEEE Photon. Technol. Lett.*, vol. 27, no. 6, pp. 577–580, Mar. 2015.
- [24] E. Haglund *et al.*, "30 GHz bandwidth 850 nm VCSEL with sub-100 fJ/bit energy dissipation at 25–50 Gbit/s," *Electron. Lett.*, vol. 51, no. 14, pp. 1096–1098, Jul. 2015.
- [25] K.-L. Chi *et al.*, "Single-mode 850-nm VCSELs for 54-Gb/s ON-OFF keying transmission over 1-km multi-mode fiber," *IEEE Photon. Technol. Lett.*, vol. 28, no. 12, pp. 1367–1370, Jun. 2016.
- [26] G. Larisch, P. Moser, J. A. Lott, and D. Bimberg, "Impact of photon lifetime on the temperature stability of 50 Gb/s 980 nm VCSELs," *IEEE Photon. Technol. Lett.*, vol. 28, no. 21, pp. 2327–2330, Nov. 2016.
- [27] E. Simpanen *et al.*, "1060 nm single-mode vertical-cavity surface-emitting laser operating at 50 Gbit/s data rate," *Electron. Lett.*, vol. 53, no. 13, pp. 869–871, Jun. 2017.
- [28] N. Ledentsov, Jr. *et al.*, "Temperature stable oxide-confined 850 nm VCSELs operating at bit rates up to 25 Gbit/s at 150 °C," in *Proc. SPIE*, Feb. 2018, Art. no. 105520P.
- [29] L. Chorchos *et al.*, "Energy efficient 850 nm VCSEL based optical transmitter and receiver link capable of 80 Gbit/s NRZ multi-mode fiber data transmission," *J. Lightw. Technol.*, vol. 38, no. 7, pp. 1747–1752, Apr. 2020.
- [30] K. Szczerba *et al.*, "30 Gbps 4-PAM transmission over 200 m of MMF using an 850 nm VCSEL," *Opt. Exp.*, vol. 19, no. 26, pp. B203–B208, Dec. 2011.
- [31] K. Szczerba, P. Westbergh, M. Karlsson, P. A. Andrekson, and A. Larsson, "60 Gbits error-free 4-PAM operation with 850 nm VCSEL," *Electron. Lett.*, vol. 49, no. 15, pp. 953–955, Jul. 2013.
- [32] T. Zuo, L. Zhang, E. Zhou, G. N. Liu, and X. Xu, "112-Gb/s duobinary 4-PAM transmission over 200-m multi-mode fibre," in *Proc. Eur. Conf. Opt. Commun.*, Valencia, Spain, Sep. 27–Oct. 1, 2015, Paper 0730.
- [33] J. M. Castro *et al.*, "200m 2x50 Gb/s PAM-4 SWDM transmission over wideband multimode fiber using VCSELs and pre-distortion signaling," in *Proc. Opt. Fiber Commun.*, Anaheim, CA, USA, Mar. 20–24, 2016, Paper Tu2G.2.
- [34] K. Szczerba, T. Lengyel, M. Karlsson, P. A. Andrekson, and A. Larsson, "94-Gb/s 4-PAM using an 850-nm VCSEL, pre-emphasis, and receiver equalization," *IEEE Photon. Technol. Lett.*, vol. 28, no. 22, pp. 2519–2521, Nov. 2016.
- [35] S. M. R. Motaghianezam *et al.*, "180 Gbps PAM4 VCSEL transmission over 300 m wideband OM4 fibre," in *Proc. Opt. Fiber Commun.*, Anaheim, CA, USA, Mar. 20–24, 2016, Paper Th3G.2.
- [36] G. Stepniak *et al.*, "Up to 108 Gb/s PAM 850 nm multi and single mode vcsel transmission over 100 m of multi mode fiber," in *Proc. Eur. Conf. Opt. Commun.*, Dusseldorf, Germany, Sep. 18–22, 2016, pp. 839–841.
- [37] F. Karinou, N. Stojanovic, C. Prodaniuc, Z. Qiang, and T. Dippon, "112 Gb/s PAM-4 optical signal transmission over 100-m OM4 multimode fiber for high-capacity data-center interconnects," in *Proc. Eur. Conf. Opt. Commun.*, Dusseldorf, Germany, Sep. 18–22, 2016, pp. 124–126.
- [38] H.-Y. Kao *et al.*, "Modal linewidth dependent transmission performance of 850-nm VCSELs with encoding PAM-4 over 100-m MMF," *IEEE J. Quantum Electron.*, vol. 53, no. 5, Oct. 2017, Art. no. 8000408.
- [39] J. Lavrencik, S. Varughese, J. S. Gustavsson, E. Haglund, A. Larsson, and S. E. Ralph, "Error-free 100Gbps PAM-4 transmission over 100m wideband fiber using 850nm VCSELs," in *Proc. Eur. Conf. Opt. Commun.*, Gothenburg, Sweden, Sep. 17–21, 2017, doi: [10.1109/ECOC.2017.8346162](https://doi.org/10.1109/ECOC.2017.8346162).
- [40] H.-Y. Kao *et al.*, "Single-mode VCSEL for pre-emphasis PAM-4 transmission up to 64 Gbit/s over 100–300 m in OM4 MMF," *Photon. Res.*, vol. 6, no. 7, pp. 666–673, Jul. 2018.

- [41] Q. Zhang *et al.*, "137 Gb/s PAM-4 transmissions at 850 nm over 40 cm optical backplane with 25 g devices with improved neural network-based equalization," *Appl. Sci.*, vol. 9, no. 23, Dec. 2019, Art. no. 5095.
- [42] L. Sun *et al.*, "Intelligent 2-dimensional soft decision enabled by k-means clustering for VCSEL-based 112-Gbps PAM-4 and PAM-8 optical interconnection," *J. Lightw. Technol.*, vol. 37, no. 24, pp. 6133–6149, Dec. 2019.
- [43] L. Sun, J. Du, K. Xu, B. Liu, and Z. He, "Enabling equalization and soft decision by k-Means for VCSEL-based PAM-4 optical interconnection," *IEEE Photon. J.*, vol. 11, no. 4, Aug. 2019, Art. no. 7203711.
- [44] J. Lavrencik *et al.*, "Error-free 100 Gbps PAM-4 transmission over 100m OM5 MMF using 1060nm VCSELS," in *Proc. Opt. Fiber Commun.*, San Diego, CA, USA, Mar. 3-7, 2019, Paper M1F.3.
- [45] J. Lavrencik, S. Varughese, N. Ledentsov Jr., L. Chorchos, N. N. Ledentsov, and S. E. Ralph, "168Gbps PAM-4 multimode fiber transmission through 50m using 28GHz 850nm multimode VCSELS," in *Proc. Opt. Fiber Commun.*, San Diego, CA, USA, Mar. 8-12, 2020, Paper W1D.3.
- [46] C.-Y. Huang *et al.*, "Comparison on OM5-MMF and OM4-MMF data links with 32-GBaud PAM-4 modulated few-mode VCSEL at 850 nm," *J. Lightw. Technol.*, vol. 38, no. 3, pp. 573–582, Feb. 2020.
- [47] T. Zuo, T. Zhang, S. Zhang, and L. Liu, "Single-lane 200-Gbps PAM-4 transmission for datacenter intra-connections employing 850-nm VCSEL," in *Proc. Asia Commun. Photon. Conf.*, Beijing, China, Oct. 24-27, 2020, Paper S3H.2.
- [48] W.-C. Lo *et al.*, "Effect of chirped dispersion and modal partition noise on multimode VCSEL encoded with NRZ-OOK and PAM-4 formats," *IEEE J. Sel. Top. Quantum Electron.*, vol. 28, no. 1, Jan./Feb. 2022, Art. no. 1500409.
- [49] M.-J. Li *et al.*, "Single-mode VCSEL transmission for short reach communications," *J. Lightw. Technol.*, vol. 39, no. 4, pp. 868–880, Feb. 2021.
- [50] N. Ledentsov *et al.*, "Narrow spectrum VCSEL development for high performance 100G transceivers and increased transmission distance over multimode fiber," *Proc. SPIE*, vol. 11704, Mar. 2021, Art. no. 117040P.
- [51] S. C. J. Lee *et al.*, "24-Gb/s transmission over 730 m of multimode fiber by direct modulation of an 850-nm VCSEL using discrete multi-tone modulation," in *Proc. Opt. Fiber Commun.*, Anaheim, CA, USA, Mar. 25-29, 2007, Paper PDP6.
- [52] S. C. J. Lee, F. Breyer, S. Randel, D. Cárdenas, H. P. A. van den Boom, and A. M. J. Koonen, "Discrete multitone modulation for high-speed data transmission over multimode fibers using 850-nm VCSEL," in *Proc. Opt. Fiber Commun.*, San Diego, CA, USA, Mar. 22-26, 2009, Paper OWM2.
- [53] M. I. Olmedo, T. A., T. Zuo, J. Estaran, X. Xu, and I. T. Monroy, "Towards 100 Gbps over 100m MMF using a 850nm VCSEL," in *Proc. Opt. Fiber Commun.*, San Francisco, CA, USA, Mar. 9-13, 2014, Paper M2E.5.
- [54] I.-C. Lu *et al.*, "Nonlinear compensation for 980 nm high power, single-mode VCSELS for energy efficient OM4 fiber transmission," in *Proc. Opt. Fiber Commun.*, San Francisco, CA, USA, Mar. 9-13, 2014, Paper Th4G.5.
- [55] I.-C. Lu *et al.*, "Very high bit-rate distance product using high-power single-mode 850-nm VCSEL with discrete multitone modulation formats through OM4 multimode fiber," *IEEE J. Sel. Top. Quantum Electron.*, vol. 21, no. 6, Nov./Dec. 2015, Art. no. 1701009.
- [56] W. A. Ling, I. Lyubomirsky, R. Rodes, H. M. Daghighian, and C. Kocot, "Single-channel 50G and 100G discrete multitoned transmission with 25G VCSEL technology," *J. Lightw. Technol.*, vol. 33, no. 4, pp. 761–767, Feb. 2015.
- [57] R. Puerta *et al.*, "107.5 Gb/s 850 nm multi- and single-mode VCSEL transmission over 10 and 100 m of multi-mode fiber," in *Proc. Opt. Fiber Commun.*, Anaheim, CA, USA, Mar. 20-24, 2016, Paper Th5B.5.
- [58] W. Bo *et al.*, "Single-lane 112 Gbps transmission over 300 m OM4 multimode fiber based on a single-transverse-mode 850nm VCSEL," in *Proc. Eur. Conf. Opt. Commun.*, Dusseldorf, Germany, Sep. 18-22, 2016, pp. 1148–1150.
- [59] C.-T. Tsai *et al.*, "Multi-mode VCSEL chip with high-indium-density InGaAs/AlGaAs quantum-well pairs for QAM-OFDM in multi-mode fiber," *IEEE J. Quantum Electron.*, vol. 53, no. 4, Aug. 2017, Art. no. 2400608.
- [60] H.-Y. Kao *et al.*, "Comparison of single-/few-/multi-mode 850 nm VCSELS for optical OFDM transmission," *Opt. Exp.*, vol. 25, no. 14, pp. 16347–16363, Jul. 2017.
- [61] C. Kottke, C. Caspar, V. Jungnickel, R. Freund, M. Agustin, and N. N. Ledentsov, "High speed 160 Gb/s DMT VCSEL transmission using pre-equalization," in *Proc. Opt. Fiber Commun.*, Los Angeles, CA, USA, Mar. 19-23, 2017, Paper W4I.7.
- [62] C. Kottke *et al.*, "High-speed DMT and VCSEL-based MMF transmission using pre-distortion," *J. Lightw. Technol.*, vol. 36, no. 2, pp. 168–174, Jan. 2018.
- [63] H.-Y. Kao *et al.*, "Long-term thermal stability of single-mode VCSEL under 96-Gbit/s OFDM transmission," *IEEE J. Sel. Top. Quantum Electron.*, vol. 25, no. 6, Nov./Dec. 2019, Art. no. 1500609.
- [64] W.-L. Wu *et al.*, "Error-free 100 GBPS PAM-4 transmission over 100m OM5 MMF using 1060nm VCSELS," in *Proc. Opt. Fiber Commun.*, San Diego, CA, USA, Mar. 3-7, 2019, Paper Tu3A.3.
- [65] C.-Y. Huang *et al.*, "Comparison of high-speed PAM4 and QAM-OFDM data transmission using single-mode VCSEL in OM5 and OM4 MMF links," *IEEE J. Sel. Top. Quantum Electron.*, vol. 26, no. 4, Jul./Aug. 2020, Art. no. 1500210.
- [66] C.-Y. Huang *et al.*, "Temperature and noise dependence of tri-mode VCSEL carried 120-Gbit/s QAM-OFDM data in back-to-back and OM5-MMF links," *J. Lightw. Technol.*, vol. 38, no. 24, pp. 6746–6758, Dec. 2020.
- [67] C.-Y. Huang, H.-Y. Wang, C.-Y. Peng, C.-T. Tsai, C.-H. Wu, and G.-R. Lin, "Multimode VCSEL enables 42-GBaud PAM-4 and 35-GBaud 16-QAM OFDM for 100-m OM5 MMF data link," *IEEE Access*, vol. 8, pp. 36363–36973, Feb. 2020.
- [68] Y.-H. Lin, C.-T. Tsai, W.-L. Wu, C.-H. Cheng, K. D. Choquette, and G.-R. Lin, "Photonic crystal structured multi-mode VCSELS enabling 92-Gbit/s QAM-OFDM transmission," *J. Lightw. Technol.*, vol. 39, no. 13, pp. 4331–4340, Jul. 2021.
- [69] N. Bamiedakis, X. Dong, D. G. Cunningham, I. H. White, and R. V. Penty, "Single-lane >100 Gb/s CAP-based data transmission over VCSEL-MMF links using low-complexity equalization," in *Proc. SPIE*, vol. 11712, Mar. 2021, Art. no. 117120L.
- [70] N. Ledentsov Jr. *et al.*, "Serial data transmission at 224 Gbit/s applying directly modulated 850 and 910 nm VCSELS," *Electron. Lett.*, to be published, doi: [10.1049/el2.12236](https://doi.org/10.1049/el2.12236).
- [71] D. J. F. Barros and J. M. Kahn, "Comparison of orthogonal frequency-division multiplexing and ON-OFF keying in direct-detection multimode fiber links," *J. Lightw. Technol.*, vol. 29, no. 15, pp. 2299–2309, Aug. 2011.
- [72] K. Kurihara, T. Numai, I. Ogura, A. Yasuda, M. Sugimoto, and K. Kasahara, "Reduction in the series resistance of the distributed bragg reflector in vertical cavities by using quasi-graded superlattices at the heterointerfaces," *J. Appl. Phys.*, vol. 73, no. 1, pp. 21–27, Jan. 1993.
- [73] Y.-C. Chang and L. A. Coldren, "Optimization of VCSEL structure for high-speed operation," in *Proc. IEEE Int. Semicond. Laser Conf.*, Sorrento, Italy, Sep. 14-18, 2008, Paper ThA1.
- [74] P. Westbergh *et al.*, "High-speed oxide confined 850-nm VCSELS operating error free at 40 Gbit/s up to 85 °C," *IEEE Photon. Technol. Lett.*, vol. 25, no. 8, pp. 768–771, 2013.
- [75] P. Moser, J. A. Lott, and D. Bimberg, "Energy efficiency of directly modulated oxide-confined high bit rate 850-nm VCSELS for optical interconnects," *IEEE J. Sel. Top. Quantum Electron.*, vol. 19, no. 4, Jul./Aug. 2013, Art. no. 1702212.
- [76] T.-H. Hsueh, H.-C. Kuo, F.-I. Lai, L.-H. Lai, and S.-C. Wang, "High-speed characteristics of large-area single-transverse-mode vertical-cavity surface-emitting lasers," *Electron. Lett.*, vol. 39, no. 21, pp. 1519–1521, Oct. 2003.
- [77] S. K. Antapurkar, A. Pandey, and K. K. Gupta, "GFDM performance in terms of BER, PAPR and OOB and comparison to OFDM system," *AIP Conf. Proc.*, vol. 1715, no. 1, Mar. 2016, Art. no. 020039.
- [78] G. Fettweis, M. Krondorf, and S. Bittner, "GFDM-generalized frequency division multiplexing," in *Proc. 69th IEEE Veh. Technol. Conf.*, Barcelona, Spain, Apr. 26-29, 2009, pp. 1–4.
- [79] N. Michailow *et al.*, "Generalized frequency division multiplexing for 5th generation cellular networks," *IEEE Trans. Commun.*, vol. 62, no. 9, pp. 3045–3061, Sep. 2014.
- [80] L. R. Rabiner, "Techniques for designing finite-duration impulse-response digital filters," *IEEE Trans. Commun. Technol.*, vol. CT-19, no. 2, pp. 188–195, Feb. 1971.
- [81] Y.-C. Chi, D.-H. Hsieh, C.-T. Tsai, H.-Y. Chen, H.-C. Kuo, and G.-R. Lin, "450-nm GaN laser diode enables high-speed visible light communication with 9-Gbps QAM-OFDM," *Opt. Exp.*, vol. 23, no. 10, pp. 13051–13059, May 2015.